Lumbar Bone Marrow Microcirculation Measurements from Dynamic Contrast-Enhanced Magnetic Resonance Imaging Is a Predictor of Event-Free Survival in Progressive Multiple Myeloma

Jens Hillengass,[1] Klaus Wasser,[6] Stefan Delorme,[2] Fabian Kiessling,[3] Christian Zechmann,[2] Axel Benner,[4] Hans-Ulrich Kauczor,[2] Anthony D. Ho,[1] Hartmut Goldschmidt,[1,5] and Thomas M. Moehler[1]

Abstract

Purpose: Dynamic contrast-enhanced magnetic resonance imaging (DCE-MRI) with high temporal resolution enables the detection of microcirculation variables amplitude A and exchange rate constant k_{ep}. In this study, the prognostic value of the DCE-MRI variables for overall survival and event-free survival in patients with progressive multiple myeloma was investigated.

Experimental Design: Between 1999 and 2001, 65 patients with progressive or relapse of multiple myeloma requiring therapy were investigated with DCE-MRI of the lumbar spine before start of therapy. The contrast uptake was quantified using a two-compartment model with the output variables amplitude A and exchange rate constant k_{ep} reflecting bone marrow microcirculation. The estimated median follow-up was 56 months. Event-free survival and overall survival were investigated for DCE-MRI variables and for established prognosis variables (β_2-microglobulin, lactate dehydrogenase, albumin, and age).

Results: Using a multivariate Cox regression model, β_2-microglobulin and amplitude A of DCE-MRI were identified as statistically significant prognostic variable of event-free survival with Ps of 0.01 and 0.02, respectively. A statistical correlation of DCE-MRI variables with overall survival could not be found. The multivariate analysis of β_2-microglobulin, age, lactate dehydrogenase, and albumin revealed β_2-microglobulin as statistically significant prognostic factor for overall survival in this group of patients ($P < 0.001$).

Conclusions: This analysis identifies contrast-enhanced DCE-MRI variable amplitude A reflecting increased bone marrow microcirculation and angiogenesis as a novel and possibly useful prognostic factor in patients with multiple myeloma. Prospective studies are currently done to further investigate this functional variable for prognosis and stratification of myeloma patients.

Recent studies have shown that increased angiogenesis is an adverse prognostic variable in patients with hematologic malignancies, including patients with multiple myeloma (1–4). Moreover, angiogenesis and endothelial activation are considered to contribute to myeloma progression. Targeting angiogenesis, therefore, became a therapeutic strategy for multiple myeloma in recent years, which thus far led to the discovery of the therapeutic activity of thalidomide and analogues in multiple myeloma (5–7).

Immunohistologic evaluation is considered as "gold standard" for the detection and quantification of angiogenesis but has several limitations because it does not reflect blood vessel permeability and is associated with a considerable sampling error. For the regular clinical situation, histologic evaluation can only be done from distinct anatomic areas (e.g., pelvis) and can not be repeated without clear clinical indication. Dynamic contrast-enhanced MRI (DCE-MRI) is a noninvasive technique for the detection of microcirculation in malignant tissues. By this method, changes of contrast enhancement are measured over a time period and described by a signal intensity-time curve. During the last decade, this method has been used with different technical approaches to characterize malignant solid tumors and to monitor their therapeutic response (8–13). In recent years, DCE-MRI has also become more important for investigation of bone marrow in patients with multiple myeloma (14, 15). In contrast to solid tumors, initial classification and prognostic assessment as well as therapeutic response of multiple myeloma cannot be based on the measurement of the tumor size. Therefore, additional radiological information has to be taken into account (e.g., the

Authors' Affiliations: [1]Department of Hematology, Oncology, and Rheumatology, University of Heidelberg; Departments of [2]Radiology and [3]Physics in Radiology and [4]Central Unit of Biostatistics, German Cancer Research Center, [5]National Center of Tumor Diseases, Heidelberg, Germany; and [6]Department of Clinical Radiology, University Hospital of Mannheim, Mannheim, Germany

Received 1/10/06; revised 8/13/06; accepted 9/28/06.

The costs of publication of this article were defrayed in part by the payment of page charges. This article must therefore be hereby marked *advertisement* in accordance with 18 U.S.C. Section 1734 solely to indicate this fact.

Note: J. Hillengass and K. Wasser contributed equally to this work.

Requests for reprints: Jens Hillengass, Department of Hematology, Oncology, and Rheumatology, University of Heidelberg, Im Neuenheimer Feld 410, 69120 Heidelberg, Germany. Phone: 1149-6221-56-8001; Fax: 11-01149-6221-56-5908; E-mail: Jens.Hillengass@med.uni-heidelberg.de.

doi:10.1158/1078-0432.CCR-06-0061

functional information obtained by DCE-MRI). A DCE-MRI protocol with high temporal resolution, as we used in our study, enables a quantification of signal intensity-time curves and the calculation of microcirculation variables. These variables are color coded and superimposed onto conventional magnetic resonance images to combine morphologic and functional information. This special procedure of DCE-MRI has already been described and applied in previous studies. The two DCE-MRI–derived microcirculation variables amplitude A and exchange rate constant k_{ep} reflect the degree of change in microcirculation (8–12, 14, 16, 17). These variables are significantly increased in patients with multiple myeloma compared with healthy controls and correlate with osteolytic bone involvement (14, 17). Increased angiogenesis and the degree of myeloma bone marrow infiltration as determined by histologic assessment of bone marrow biopsies are significantly correlated with an increased amplitude A of DCE-MRI (17, 18). Furthermore, amplitude A was found to be predictive for local complications as vertebral collapse by Scherer et al. (18).

This is the first analysis investigating the prognostic relevance of DCE-MRI microcirculation variables for event-free survival and overall survival of patients with progressive multiple myeloma.

Materials and Methods

Patients. Between 1999 and 2001, 65 patients with relapsed, refractory (n = 60), or newly diagnosed (n = 5) multiple myeloma requiring systemic therapy according to international standards were investigated with DCE-MRI of the lumbar spine using a study protocol approved by the institutional ethics committee. All patients gave written informed consent. Patient characteristics are listed in Table 1. Detailed description of DCE-MRI data for a subset of patients included in this retrospective analysis was published previously (14, 19). In all cases, DCE-MRI was done after confirmed relapse or progressive disease of multiple myeloma before the onset of systemic therapy, including application of corticosteroids, because changes in bone marrow signal after response to treatment have been described (13, 14). For the same reason, patients with prior radiotherapy of the lumbar spine were excluded from the study.

Table 1. Patient demographic and disease characteristics (N = 65)

Characteristic	n (%)
Female sex	26 (40)
Death during observation period	34 (52.3)
Age >60y	22 (33.8)
Monoclonal protein	
Bence Jones	4 (6.2)
IgA	21 (32.3)
IgG	39 (60)
IgG + IgA	1 (1.5)
Refractory or relapsed*	60 (92.3)
Duration of disease > 60 mos*	18 (27.7)
Prior high-dose chemotherapy	45 (69.2)
Subsequent therapy TCED	25 (38.5)
Serum β_2-microglobulin > 2.5 mg/L (n = 60)†	36 (60)
Plasma creatinine > 1.3 mg/dL (n = 60)†	2 (3.3)
Plasma calcium > 2.65 mmol/L (n = 60)†	0 (0)
Durie/Salmon stage III	56 (86.2)
Plasma LDH > 240 units/L (n = 58)†	2 (3.4)
Hemoglobin < 9 mg/dL (n = 60)	7 (11.7)

Abbreviations: TCED, thalidomide/cyclophosphamide/etoposide/dexamethasone; LDH, lactate dehydrogenase.
*At time of DCE-MRI.
†Upper level of normal controls for selected laboratory tests: serum β_2-microglobulin (2.5 mg/L), plasma lactate dehydrogenase (240 units/L), plasma calcium (2.65 mmol/L), plasma creatinine (1.3 mg/dL).

All patients in this evaluation received a thalidomide containing regimen subsequent to DCE-MRI. Forty-one patients (63% of patients) were treated with thalidomide as single agent with daily application of up to 400 mg thalidomide dependent on the individual tolerability of thalidomide. This therapeutic approach and results have been previously presented (20).

Twenty-four patients (37% of patients) were treated with a combination therapy of oral thalidomide (up to 400 mg), oral dexamethasone (40 mg, days 1-4), i.v. cyclophosphamide (400 mg/kg/body weight), and i.v. etoposide (40 mg/kg/body weight) of a 28- to 35-day cycle as reported previously (21).

Depending on the outcome of thalidomide or thalidomide/cyclophosphamide/etoposide/dexamethasone chemotherapy, further treatment was done in case of relapse at the discretion of the responsible physicians.

The control group consisted of two different parts. The details about these groups have been introduced in previous studies. (a) Lumbar spine of healthy volunteers (n = 16/10; median age, 54/35 years; refs. 14, 19). (b) Pelvic bone of multiple myeloma patients, whose bone marrow biopsies were free of pathologic plasma cell infiltration (n = 8; mean age, 56 years; ref. 17).

Overall survival and event-free survival were updated for all patients in February 2005. The reference date for survival was the date of DCE-MRI. The cutoff for survival information was December 31, 2004. The estimated median follow-up calculated from time point of MRI was 56 months (95% confidence interval, 50-62 months). Patients with irradiation of the lumbar spine were excluded from the study.

DCE-MRI protocol. The principles of the DCE-MRI protocol and the post-processing have been described previously (8, 16, 22). All examinations were done on a 1.5-T Tomograph (Vision, Siemens, Erlangen, Germany) with a spine coil. First, the lower spinal column from the 12th thoracic vertebra to the sacrum was examined with a sagittal STIR, T2w flash 2D, and T1wSE. The following DCE-MRI of the same region consisted in a Saturation-recovery-Turbo FLASH-Sequence (TR/TE: 7.0/3.9 ms, flip angle: 15 degrees, T_{rec} = 250 ms, matrix: 256 × 128, interpolated to 256 × 256, slice thickness: 5 mm) in sagittal orientation. The total measurement time of DCE-MRI was 5.5 min, consisting in 22 acquisitions of image stacks of 15 images each, with a resulting cycle time of 15.21 s. The head-feet directed field of view routinely covered the lumbar spine, including the lower thoracic spine up to Th10 without regard to any seen lesions on T1 or T2w images.

The effect of operator dependency on injection times was reduced by a short constant rate infusion using a variable-speed infusion pump (Tomojet, Bruker, Basel, Switzerland). As contrast medium, 0.1 mmol/kg gadolinium-diethylenetriaminepentaacetic acid (Magnevist, Schering, Berlin, Germany) was injected over 30 s, starting with the second measurement. At the end of the examination, another sagittal T1wSE sequence followed.

Data of DCE-MRI were analyzed on a Vax Alpha 3000/500 workstation (DEC, Maynard, MA) with a self-developed software by Hoffmann et al. (8).

In each pixel, the detected signal intensity-time course was overlaid by a graph, which calculation was based on the so-called two-compartment model proposed by Brix et al. (22). The signal-time curve was fitted by using a "Levenberg-Marquart" algorithm. The model assumes a constant infusion rate of the contrast medium into a central (intravascular) compartment and an exchange of the contrast medium between the central and another, peripheral (extravascular, extracellular) compartment.

The tissue-specific information contained in DCE-MRI–based signal intensity-time courses is described by two relevant model variables: amplitude A (a.U.), which is proportional to the relative signal enhancement, and the exchange rate constant k_{ep} (min^{-1}) reflecting the contrast agent transit between the extravascular and intravascular compartment. Using a two-parametric 16-color map (Fig. 1) encoding for both variables amplitude A and exchange rate constant k_{ep}, each pixel was assigned a color, and the resulting color map was overlaid on the morphologic magnetic resonance images.

Image analysis. Changes of signal enhancement and distribution of pharmacokinetic variables as viewed by color-coded DCE-MRI images were classified based on visual aspects as "diffuse," "focal," "mixed," and "normal," according to previous studies (15, 23–25). A "diffuse" pattern was characterized by an extensive and non-circumscribed signal increase mostly resulting in a pink color in the color-coded variable maps (ranges of amplitude A and exchange rate constant k_{ep} that define a specific color are listed in Fig. 1). A "focal" pattern was characterized by a circumscribed signal increase. These "hotspots" were visualized as white, yellow, or green colors in the DCE-MRI variable maps. Another pattern was classified as "mixed" ("focal" and "diffuse"). In a fourth group of patients, no signal changes were found compared with normal bone marrow of lumbar spine or pelvic bone, examined in previous studies (14, 17). MRI maps of those patients were classified as "normal."

Subsequently, a systematic analysis of a manually drawn region of interest (ROI) was carried out. For this ROI, the software automatically calculated mean signal intensities on single images and then created curves where the mean signal intensity in the ROI was plotted over time; amplitude A and exchange rate constant k_{ep} were calculated for this curve. The ROI was inserted depending on the pattern (see below) of the DCE-MR image. In patients showing a "diffuse" or "normal" pattern, two vertebra were analyzed. In those cases, the ROI included nearly the complete anatomic vertebra, excluding the endplates and the basis of the vertebral vein plexus. The ROIs were positioned in the midline at the center of the coil. In patients with a "focal" pattern, two reference lesions were selected for ROI analysis; the ROI was covering the whole lesion. In "mixed" patterns, only the focal lesions were investigated.

Statistical analysis. In this study, two pairs of values for amplitude A and exchange rate constant k_{ep} out of two ROIs of the lumbar spine were detected as explained above. The calculation was done for the mean value of each variable.

To examine the prognostic value of the variables amplitude A and exchange rate constant k_{ep} of DCE-MRI, we used the proportional hazards model as proposed by Cox (26).

The effects of the DCE-MRI variables, taking into account the established clinical prognostic factors β_2-microglobulin, albumin, lactate dehydrogenase, age, and duration of disease, were analyzed by using a backward selection as proposed by Lawless and Singhal (27) for the search for a model and bootstrap resampling using 200 samples for validation of the model. A Somer's D rank correlation between predicted survival probability and observed survival time and the slope shrinkage characterizing the degree of "over adaptation" by the search for a model were calculated. Finally, the 200 bootstrap samples were used to evaluate the selection frequency of each factor in the backward selection process.

Correlations of the DCE-MRI variables and established prognostic markers of multiple myeloma were examined by using Spearman's rho test.

To illustrate the results of the Cox regression model, predicted event-free survival and overall survival were calculated.

Results

Description of DCE-MRI results. The median of amplitude A was 0.42 (range, 0-1.18), and the median of the exchange rate constant k_{ep} was 3.89 (range, 0-7.98).

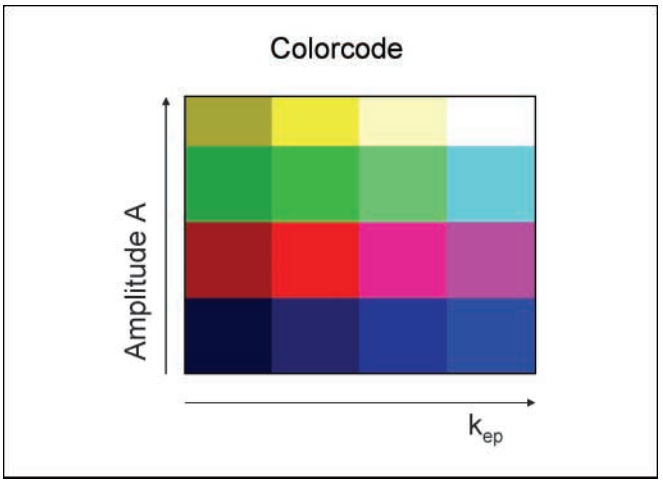

Fig. 1. Two-dimensional color scale that is used for encoding the variables amplitude A and exchange rate constant k_{ep}. Each of the 16 different colors represents a discrete interval of amplitude A (0.1-0.4, 0.4-0.8, 0.8-1.2, and >1.2) and exchange rate constant k_{ep} (0-1.6, 1.6-3.2, 3.2-48, and >4.8).

The analysis of the color-coded DCE MRI images (color maps) revealed four different patterns of microcirculation as described in Materials and Methods. A "normal" pattern (Fig. 2A), as it was found in healthy controls, was identified in 26 patients (40%). A "diffuse" pattern (Fig. 2B) was found in 22 patients (34%), and a "focal" pattern (Fig. 2C) was observed in 12 patients (18%). Furthermore, a "mixed" pattern showing a combination of "diffuse" and "focal" pattern was noted in 5 patients (8%). No statistically significant prognostic effect based on these different patterns could be found.

DCE-MRI variables and event-free survival. A total of 51 events (death or progression) were recorded. Event-free survival time was defined as time from DCE-MRI until death or progression. During the observation time, 47 patients had progressive disease. Thirty-four patients died, and the cause of death was progressive disease in 32 patients, graft-versus-host disease after allogeneic transplantation in 1 patient, and intestinal bleeding due to newly diagnosed gallbladder carcinoma in 1 patient.

The median overall survival was 49.5 months (95% confidence interval, 40 to infinity), and the median event-free survival was 17 months (95% confidence interval, 12-25). The estimated event-free survival and overall survival for the whole group of patients are shown in Fig. 3.

Using a multivariate Cox model, the DCE-MRI variables amplitude A and exchange rate constant k_{ep} were investigated with additional factors known to have prognostic value in multiple myeloma (albumin, lactate dehydrogenase, β_2-microglobulin, age, and duration of disease). The proportional hazards regression model for event-free survival with backward selection identified only two significant prognostic factors: the DCE-MRI variable amplitude A (P = 0.02) and β_2-microglobulin (P = 0.01). No statistically significant effect of the exchange rate constant k_{ep} was found.

To illustrate the prognostic relevance of amplitude A and the interaction of amplitude A and β_2-microglobulin, the predicted event-free survival based on the upper and lower quartiles for each variable was computed. This defined four risk groups: "high-risk" group characterized by values for amplitude A and

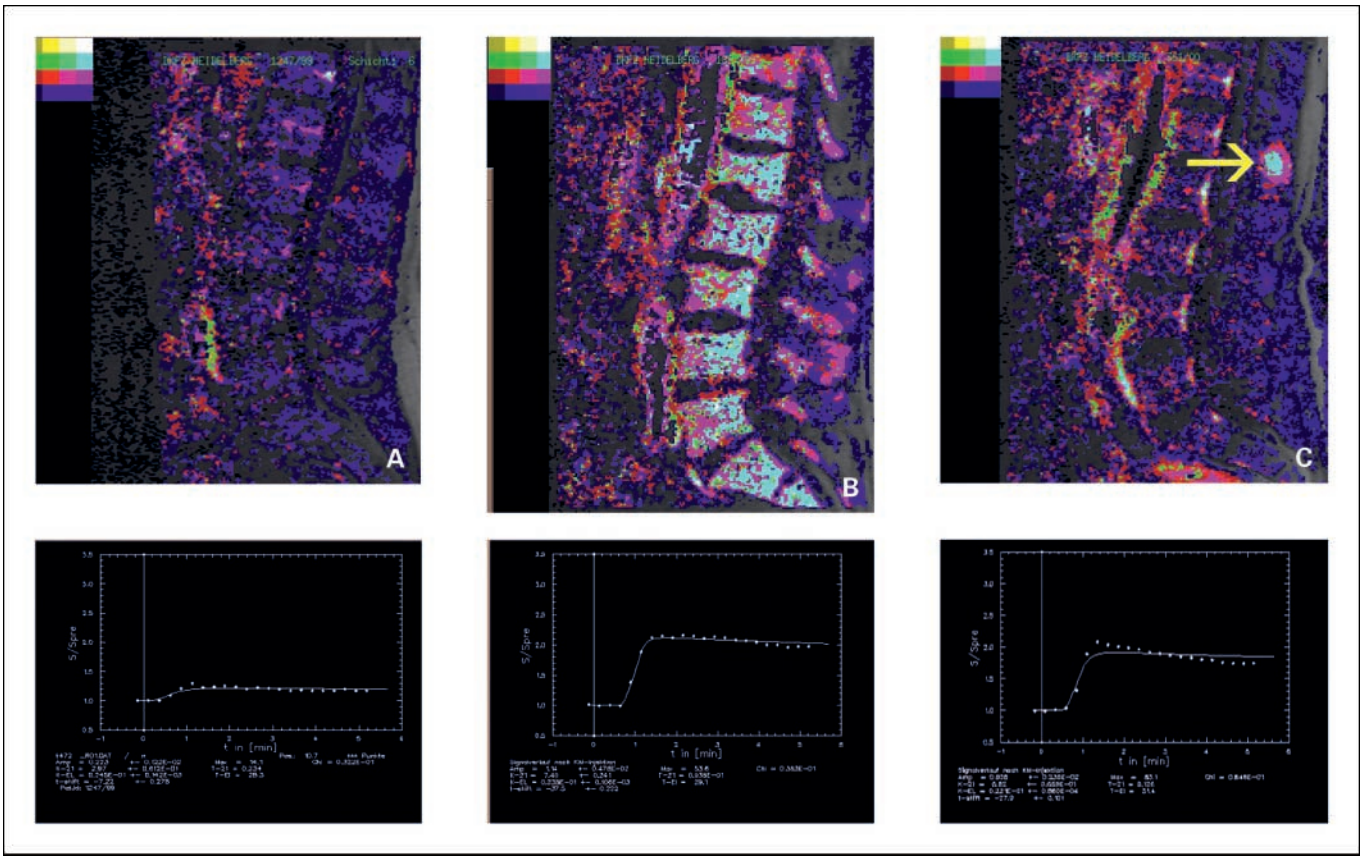

Fig. 2. Examples of color-coded maps of the lumbar spine (sagittal slices) and corresponding signal intensity-time curves obtained by ROI analysis. *A,* normal pattern of a healthy person. The color coding is homogenous and indicates low values of amplitude *A* and exchange rate constant k_{ep}. The signal intensity-time curve is characterized by a smooth shape. *B,* diffuse infiltration pattern. The color coding is inhomogeneous and indicates high values of amplitude *A* and exchange rate constant k_{ep}. The signal intensity-time curve is characterized by a steep and high increase followed by a slight decrease over time. *C,* focal infiltration of the spinosus process of the first lumbar vertebra color coding indicates high values of amplitude *A* and exchange rate constant k_{ep}. The signal intensity-time curve shows a steep and high increase followed by a slight decrease over time.

β_2-microglobulin in the upper quartile, two "intermediate-risk" groups with only one of both variables amplitude *A* and β_2-microglobulin in the upper quartile, and a "low-risk" group for lower quartiles of amplitude *A* and β_2-microglobulin distributions (Fig. 4A).

The same type of graphical illustration was applied to display the curves for predicted event-free survival of both DCE-MRI microcirculation variables. Again, four risk groups could be identified using this combined approach. As exchange rate constant k_{ep} was not a significant variable on multivariate analysis, separation of predicted event-free survival was less pronounced than using β_2-microglobulin when four risk groups were calculated in combination with amplitude *A* (Fig. 4B).

DCE-MRI variables and overall survival. Overall survival was defined as the time from DCE-MRI until death. β_2-Microglobulin ($P < 0.001$) was found to be the only statistically significant prognostic factor after backward selection of the Cox model (Table 2). Neither amplitude *A* nor exchange rate constant k_{ep} were found to correlate significantly in this group of patients with overall survival (Fig. 5A). For graphical presentation of results, again, four risk groups were defined using the distributions of the established variables lactate dehydrogenase and β_2-microglobulin as described above. Predicted overall survival was then computed for these four groups (Fig. 5B).

Discussion

The present analysis based on a long median follow-up of 4.5 years is the first to show the prognostic relevance of the DCE-MRI variable amplitude *A* for event-free survival in multiple myeloma patients.

The finding of amplitude *A* as an adverse variable for event-free survival is based on a multivariate Cox analysis. Similar to amplitude *A*, β_2-microglobulin was also identified as an independent adverse prognostic variable. β_2-Microglobulin is one of the best prognostic variables for multiple myeloma and is, together with albumin, the basis for the recently published international staging system for multiple myeloma (28). Neither the DCE-MRI variable exchange rate constant k_{ep} nor any of the other prognostic variables tested were found to be significant for event-free survival in multivariate analysis. The lack of prognostic power of the other variables, including exchange rate constant k_{ep}, may be due to a comparably low number of patients for this question. The second reason could be that we investigated patients with progressive myeloma before the start of a thalidomide-containing treatment regimen, but subgroups with increased homogeneity of patient population were too small for statistical survival analysis.

Although there was a trend indicating amplitude *A* as adverse prognostic variable for overall survival (data not shown)

multivariate analysis did not identify a statistically significant correlation for amplitude A or for exchange rate constant k_{ep} with overall survival. For all other known prognostic variables, only β_2-microglobulin was confirmed to be significant. The finding that the prognostic implication of β_2-microglobulin was confirmed in our investigation supports the idea that despite some heterogeneity in patient characteristics, we investigated a "normal" population of patients with progressive myeloma, which indicates that our findings are not restricted to our patient population. These data, therefore, initiated a prospective study to investigate the prognostic implications of the DCE-MRI variable amplitude A in untreated patients with active myeloma in our departments. We hope that our data will encourage other investigators to include DCE-MRI techniques in the work up of patients in clinical studies.

As mentioned above, this is the first study to show a prognostic effect of DCE-MRI in multiple myeloma for event-free survival reflecting *systemic* disease activity. In line with these findings, we and others have already shown that DCE-MRI–derived amplitude A is significantly correlated with *local* complications and the degree of bone destruction in multiple myeloma (14, 18). In particular, Scherer et al. could show that an increase in amplitude A is significantly correlated with collapse of respective vertebra. These data indicate that a focal DCE-MRI pattern is correlated with high amplitude A or conversely that focal involvement of bone marrow by myeloma cells is associated with more pronounced changes in microcirculation than diffuse infiltration. Although we hypothesize that focal involvement is also associated with increased amplitude A, our set of data did not show a significant correlation of a focal pattern of bone involvement by multiple myeloma with event-free survival.

Prognostic data for multiple myeloma patients generated by DCE-MRI significantly add to the already existing number of prognostic factors for multiple myeloma for several reasons. DCE-MRI represents a functional variable that reflects microcirculation and contrast uptake and is most likely associated

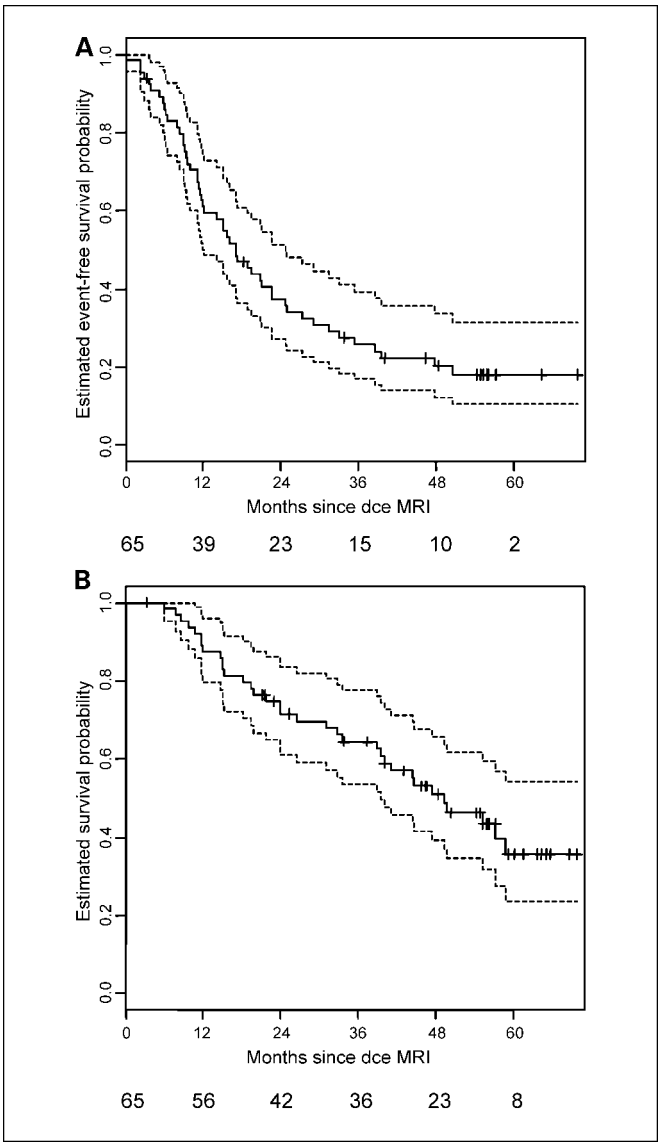

Fig. 3. Estimated event-free survival (*A*) and overall survival (*B*) in months after DCE-MRI.

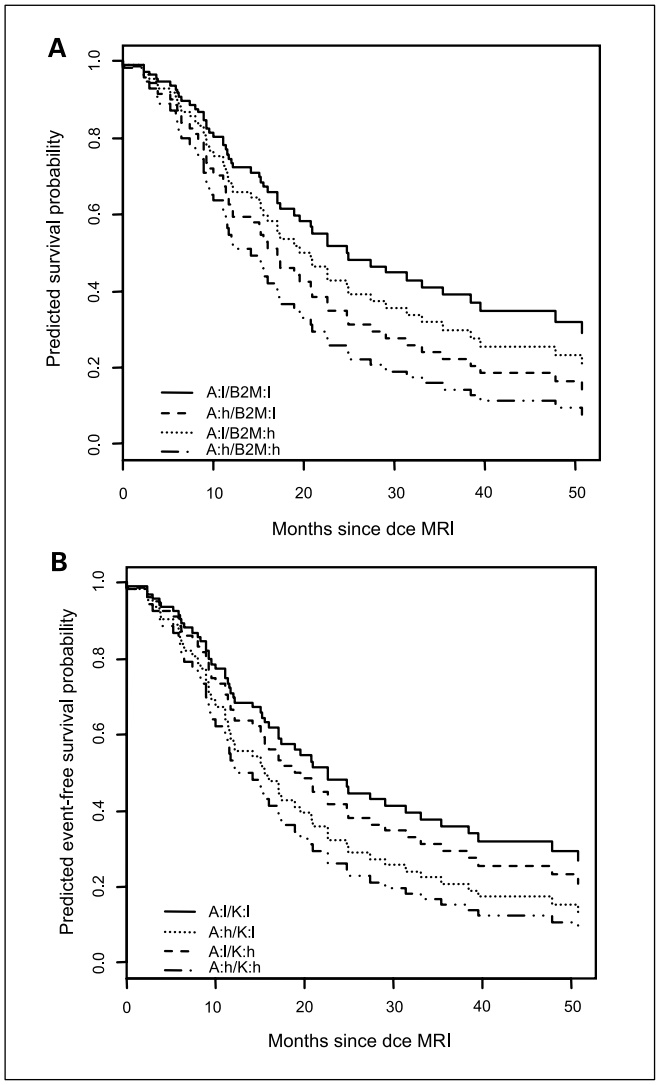

Fig. 4. Event-free survival for the amplitude A in combination with β_2-microglobulin (*B2M*; *A*) and exchange rate constant k_{ep} (*K*; *B*).

Table 2. Results of the Cox proportional hazards model

End point	Factor	Hazard ratio (95% confidence interval)	*P*	Selection frequency (%)
EFS	β_2-Microglobulin	1.13 (1.03-1.23)	0.01	77.5
	Amplitude *A*	1.62 (1.02-2.58)	0.02	64.5
OAS	β_2-Microglobulin	1.20 (1.08-1.33)	<0.001	77.5

NOTE: Hazard ratios and confidence intervals are computed for a 1-unit increment in β_2-microglobulin and a 0.5-unit increment in amplitude *A*.
Abbreviations: EFS, event-free survival; OAS, overall survival.

with disease activity. Microcirculation is correlated with increased vessel permeability and angiogenesis. Indeed, it has been shown that DCE-MRI variable amplitude *A* is strongly correlated with histologically detected microvessel density (17).

Angiogenesis detected by histopathologic examinations of bone marrow biopsies has been shown to be an adverse prognostic variable for multiple myeloma and for plasmocytomas (29, 30). Angiogenesis is considered a major factor for myeloma progression. In contrast to the histologic detection of microvessel density, DCE-MRI has the advantage of being a functional variable, providing the opportunity for subsequent examinations including a much larger area of investigation. All arguments summarized in this paragraph highlight the fact that the prognostic implications of DCE-MRI fit well into the pathophysiologic concept of myeloma progression and myeloma activity.

In recent years, new staging models for multiple myeloma have been developed. The Durie/Salmon PLUS classification, which has been developed based on the Durie/Salmon system as international standard for the last 30 years, takes into account the prognostic implications of standard MRI of the vertebral cord (31). Work by Baur-Melnyk et al., which has provided much of the scientific basis for the Durie/Salmon PLUS system, revealed that the number of focal lesions determined by MRI as well as the degree of diffuse infiltration have prominent prognostic implications, which are further increased when the standard Durie/Salmon system is combined with MRI (32). Extending the investigated region static total body MRI, which can be done by new MRI tomographs, is another important new technique.

It is very likely that DCE-MRI further adds to the prognostic implications of standard MRI. First, data implicate that DCE-MRI could be superior in determining disease activity and response to therapy (14).[6] As outlined above, microcirculation variables can be calculated according to pharmacokinetic equations and are less dependent on subjective assessment of the evaluating radiologists. It is very conceivable that both MRI techniques are complementary and can be done subsequently on one patient within one appointment. Additional time requirement of DCE-MRI after static MRI is ~7 min.

Our data indicate that further development of novel sequences, such as high temporal–resolution three-dimensional acquisition, could be valuable to improve the prognostic power of DCE-MRI for local and systemic disease activity in multiple myeloma. Another area of future development is the modification and generation of quantitative software using different mathematical models for bone marrow microcirculation. A histogram-based technique of analysis that uses and displays all pixel of a given ROI for correlative analysis should also be evaluated in future trials. The software development has to take into account that DCE-MRI will be a potential standard technique for myeloma patients in the future and has to be adapted for routine application.

A successful example for transition of DCE-MRI technique from research into clinical application is DCE-MRI in breast cancer. It has been used for detection and evaluation of breast cancer for over a decade (33). DCE-MRI in breast cancer was

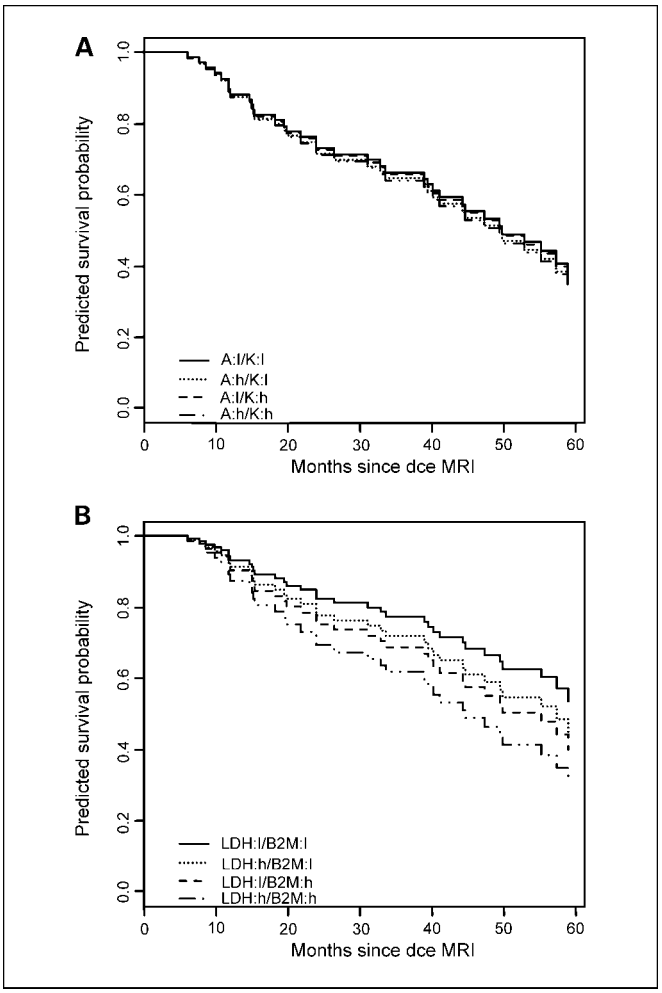

Fig. 5. Overall survival for high/low amplitude *A* in combination with exchange rate constant k_{ep} (*A*) and the combination of β_2-microglobulin and lactate dehydrogenase (*LDH*; *B*).

[6] T.M. Moehler and K. Wasser, unpublished results.

done before first publications on DCE-MRI in myeloma were published (8, 33–35). Similar to the situation in multiple myeloma, DCE-MRI images of the breast can highlight areas of increased permeability and microvascular density and thereby are useful in evaluating breast masses of unknown dignity (8, 10, 36, 37). Furthermore, this method is increasingly used for monitoring breast cancer during primary chemotherapy (11, 32). Our data on the predictive value of amplitude *A* for local complications and for event-free survival in multiple myeloma indicate that DCE-MRI is likely to develop as future and additional tool for routine work up of myeloma patients. DCE-MRI could guide clinicians in specific questions as decisions on radiotherapy of vertebra that are under high risk to collapse, giving prognostic implications on the success of a systemic therapy and evaluating asymptomatic and smoldering myeloma.

The prognostic potential of DCE-MRI might not only be restricted to an overall assessment of risk for local or systemic disease activity. In the advent of antiangiogenic drugs and other drugs targeting microcirculation, it might be useful to identify subpopulations of patients that specifically benefit from targeted therapeutic approaches. Evaluating patients with DCE-MRI within clinical trials with antiangiogenic drugs will therefore be of particular interest.

In conclusion, DCE-MRI is able to display and monitor changes in bone marrow microcirculation as consequence of myeloma-induced angiogenesis and blood vessel permeability. Our report describes the DCE-MRI–derived microcirculation variable amplitude *A* as a prognostic variable for event-free survival in progressive multiple myeloma. DCE-MRI has the potential to complement existing prognostic variables and imaging techniques in assessment of myeloma. DCE-MRI might be able to identify subpopulation of patients that profit from therapeutic approaches targeting altered microcirculation as antiangiogenic drugs.

References

1. Munshi NC, Wilson C. Increased bone marrow microvessel density in newly diagnosed multiple myeloma carries a poor prognosis. Semin Oncol 2001;28:565–9.
2. Moehler TM, Neben K, Ho AD, Goldschmidt H. Angiogenesis in hematologic malignancies. Ann Hematol 2001;80:695–705.
3. Vacca A, Ribatti D, Roncali L, Dammacco F. Angiogenesis in B cell lymphoproliferative diseases. Biological and clinical studies. Leuk Lymphoma 1995;20:27–38.
4. Vacca A, Ribatti D, Presta M, et al. Bone marrow neovascularization, plasma cell angiogenic potential, and matrix metalloproteinase-2 secretion parallel progression of human multiple myeloma. Blood 1999;93:3064–73.
5. Moehler TM, Hillengass J, Goldschmidt H, Ho AD. Antiangiogenic therapy in hematologic malignancies. Curr Pharm Des 2004;10:1221–34.
6. Strasser K, Ludwig H. Thalidomide treatment in multiple myeloma. Blood Rev 2002;16:207–15.
7. Rajkumar SV. Thalidomide in multiple myeloma. Oncology (Williston Park, NY) 2000;14:S11–6.
8. Hoffmann U, Brix G, Knopp MV, Hess T, Lorenz WJ. Pharmacokinetic mapping of the breast: a new method for dynamic MR mammography. Magn Reson Med 1995;33:506–14.
9. Hawighorst H, Weikel W, Knapstein PG, et al. Angiogenic activity of cervical carcinoma: assessment by functional magnetic resonance imaging-based parameters and a histomorphological approach in correlation with disease outcome. Clin Cancer Res 1998;4:2305–12.
10. Knopp MV, Weiss E, Sinn HP, et al. Pathophysiologic basis of contrast enhancement in breast tumors. J Magn Reson Imaging 1999;10:260–6.
11. Wasser K, Klein SK, Fink C, et al. Evaluation of neoadjuvant chemotherapeutic response of breast cancer using dynamic MRI with high temporal resolution. Eur Radiol 2003;13:80–7.
12. Hawighorst H, Knopp MV, Debus J, et al. Pharmacokinetic MRI for assessment of malignant glioma response to stereotactic radiotherapy: initial results. J Magn Reson Imaging 1998;8:783–8.
13. Rahmouni A, Divine M, Mathieu D, et al. MR appearance of multiple myeloma of the spine before and after treatment. AJR Am J Roentgenol 1993;160:1053–7.
14. Moehler TM, Hawighorst H, Neben K, et al. Bone marrow microcirculation analysis in multiple myeloma by contrast-enhanced dynamic magnetic resonance imaging. Int J Cancer 2001;93:862–8.
15. Rahmouni A, Divine M, Mathieu D, et al. Detection of multiple myeloma involving the spine: efficacy of fat-suppression and contrast-enhanced MR imaging. AJR Am J Roentgenol 1993;160:1049–52.
16. Brix G, Schreiber W, Hoffmann U, Guckel F, Hawighorst H, Knopp MV. Methodological approaches to quantitative evaluation of microcirculation in tissues with dynamic magnetic resonance tomography. Radiologe 1997;37:470–80.
17. Nosas-Garcia S, Moehler T, Wasser K, et al. Dynamic contrast-enhanced MRI for assessing the disease activity of multiple myeloma: a comparative study with histology and clinical markers. J Magn Reson Imaging 2005;22:154–62.
18. Scherer A, Wittsack HJ, Strupp C, Gattermann N, Haas R, Modder U. Vertebral fractures in multiple myeloma: first results of assessment of fracture risk using dynamic contrast-enhanced magnetic resonance imaging. Ann Hematol 2002;81:517–21.
19. Wasser K, Moehler T, Neben K, et al. Dynamic MRI of the bone marrow for monitoring multiple myeloma during treatment with thalidomide as monotherapy or in combination with CED chemotherapy. RoFo 2004;176:1285–95.
20. Neben K, Moehler T, Benner A, et al. Dose-dependent effect of thalidomide on overall survival in relapsed multiple myeloma. Clin Cancer Res 2002;8:3377–82.
21. Moehler TM, Neben K, Benner A, et al. Salvage therapy for multiple myeloma with thalidomide and CED chemotherapy. Blood 2001;98:3846–8.
22. Brix G, Semmler W, Port R, Schad LR, Layer G, Lorenz WJ. Pharmacokinetic parameters in CNS Gd-DTPA enhanced MR imaging. J Comput Assist Tomogr 1991;15:621–8.
23. Baur A, Stabler A, Steinborn M, et al. Magnetic resonance tomography in plasmacytoma: ranking of various sequences in diffuse and focal infiltration patterns. RoFo 1998;168:323–9.
24. Stabler A, Baur A, Bartl R, Munker R, Lamerz R, Reiser MF. Contrast enhancement and quantitative signal analysis in MR imaging of multiple myeloma: assessment of focal and diffuse growth patterns in marrow correlated with biopsies and survival rates. AJR Am J Roentgenol 1996;167:1029–36.
25. Rahmouni A, Montazel JL, Divine M, et al. Bone marrow with diffuse tumor infiltration in patients with lymphoproliferative diseases: dynamic gadolinium-enhanced MR imaging. Radiology 2003;229:710–7.
26. Cox DR. Regression models and life tables. J R Stat Soc 1972;34:187–220.
27. Lawless JF, Singhal K. Efficient screening of nonnormal regression models. Biometrics 1978;34:318–27.
28. Greipp PR, San Miguel J, Durie BG, et al. International staging system for multiple myeloma. J Clin Oncol 2005;23:3412–20.
29. Rajkumar SV, Leong T, Roche PC, et al. Prognostic value of bone marrow angiogenesis in multiple myeloma. Clin Cancer Res 2000;6:3111–6.
30. Andersen NF, Standal T, Nielsen JL, et al. Syndecan-1 and angiogenic cytokines in multiple myeloma: correlation with bone marrow angiogenesis and survival. Br J Haematol 2005;128:210–7.
31. Baur-Melnyk A, Buhmann S, Durr HR, Reiser M. Role of MRI for the diagnosis and prognosis of multiple myeloma. Eur J Radiol 2005;55:56–63.
32. Baur A, Stabler A, Nagel D, et al. Magnetic resonance imaging as a supplement for the clinical staging system of Durie and Salmon? Cancer 2002;95:1334–45.
33. Knopp MV, Brix G, Junkermann HJ, Sinn HP. MR mammography with pharmacokinetic mapping for monitoring of breast cancer treatment during neoadjuvant therapy. Magn Reson Imaging Clin N Am 1994;2:633–58.
34. Ercolani P, Valeri G, Amici F. Dynamic MRI of the breast. Eur J Radiol 1998;27 Suppl 2:S265–71.
35. Stack JP, Redmond OM, Codd MB, Dervan PA, Ennis JT. Breast disease: tissue characterization with Gd-DTPA enhancement profiles. Radiology 1990;174:491–4.
36. Brix G, Kiessling F, Lucht R, et al. Microcirculation and microvasculature in breast tumors: pharmacokinetic analysis of dynamic MR image series. Magn Reson Med 2004;52:420–9.
37. Furman-Haran E, Kelcz F, Degani H. Magnetic resonance imaging of breast cancer angiogenesis: a review. J Exp Clin Cancer Res 2002;21:47–54.

Clinical Cancer Research

Lumbar Bone Marrow Microcirculation Measurements from Dynamic Contrast-Enhanced Magnetic Resonance Imaging Is a Predictor of Event-Free Survival in Progressive Multiple Myeloma

Jens Hillengass, Klaus Wasser, Stefan Delorme, et al.

Clin Cancer Res 2007;13:475-481.